Article

Synthesis, Physicochemical and Biological Study of Gallium-68- and Lutetium-177-Labeled VEGF-A$_{165}$/NRP-1 Complex Inhibitors Based on Peptide A7R and Branched Peptidomimetic

Katarzyna Masłowska [1,*], Ewa Witkowska [2], Dagmara Tymecka [2] , **Paweł Krzysztof Halik [1]** , **Aleksandra Misicka [2,*]** and **Ewa Gniazdowska [1]**

[1] Centre of Radiochemistry and Nuclear Chemistry, Institute of Nuclear Chemistry and Technology, Dorodna 16, 03-195 Warsaw, Poland; p.halik@ichtj.waw.pl (P.K.H.); e.gniazdowska@ichtj.waw.pl (E.G.)

[2] Faculty of Chemistry, University of Warsaw, Pasteura 1, 02-093 Warsaw, Poland; ewawit@chem.uw.edu.pl (E.W.); dulok@chem.uw.edu.pl (D.T.)

* Correspondence: k.maslowska@ichtj.waw.pl (K.M.); misicka@chem.uw.edu.pl (A.M.)

Abstract: Neuropilin-1 (NRP-1) is a surface receptor found on many types of cancer cells. The overexpression of NRP-1 and its interaction with vascular endothelial growth factor-165 (VEGF$_{165}$) are associated with tumor growth and metastasis. Therefore, compounds that block the VEGF$_{165}$/NRP-1 interaction represent a promising strategy to image and treat NRP-1-related pathologies. The aim of the presented work was to design and synthesize radioconjugates of two known peptide-type inhibitors of the VEGF$_{165}$/NRP-1 complex: A7R peptide and its shorter analog, the branched peptidomimetic Lys(hArg)-Dab-Pro-Arg. Both peptide-type inhibitors were coupled to a radionuclide chelator (DOTA) via a linker (Ahx) and so radiolabeled with Ga-68 and Lu-177 radionuclides, for diagnostic and therapeutic uses, respectively. The synthesized radioconjugates were tested for their possible use as theranostic-like radiopharmaceuticals for the imaging and therapy of cancers that overexpress NRP-1. The obtained results indicate good efficiency of the radiolabeling reaction and satisfactory stability, at least $3t_{1/2}$ for the ^{68}Ga- and $1t_{1/2}$ for the ^{177}Lu-radiocompounds, in solutions mimicking human body fluids. However, enzymatic degradation of both the studied inhibitors caused insufficient stability of the radiocompounds in human serum, indicating that further modifications are needed to sufficiently stabilize the peptidomimetics with inhibitory properties against VEGF$_{165}$/NRP-1 complex formation.

Keywords: ^{68}Ga/^{177}Lu-radiopharmaceuticals; cancer therapy; Neuropilin-1; VEGF$_{165}$/NRP-1 complex inhibitor; A7R peptide; peptidomimetics; angiogenesis; tyrosine kinase inhibitor

1. Introduction

NRP-1 plays one of the most important roles in the development of angiogenesis, which is the formation of new blood vessels from existing ones. One of the main stages of angiogenesis is the interaction between the pro-angiogenic factor (VEGF-A$_{165}$), its receptor (VEGFR-2), and the NRP-1 co-receptor [1–7]. NRP-1 acts in two ways: it binds to the pro-angiogenic ligand VEGF-A$_{165}$ through its b1/b2 subdomains, and in parallel, it acts as a co-receptor for VEGFR-2. The resulting ternary VEGF-A$_{165}$/VEGFR-2/NRP-1 complex induces autophosphorylation of the VEGFR-2 tyrosine kinase domains, which influences cell proliferation, differentiation, migration, gene expression, and apoptotic survival of endothelial cells, which ultimately induces angiogenesis [8–10]. Many reports also indicate that NRP-1, which is found on many types of cancer cells, lacks catalytic activity and may also serve as a separate receptor for VEGF-A$_{165}$, stimulating tumor growth and metastasis. NRP-1 overexpression may also increase tumor growth and is often associated with poor prognosis, especially in tumors of epithelial origin [3,11–18]. Due to the significant role of NRP-1 in angiogenesis and the relatively well-known mechanisms of the formation and

action of the VEGF-A$_{165}$/NRP-1 complex, the design of compounds that block the formation of this complex is an interesting direction in the search for anti-angiogenic and anti-cancer drugs [4,19–25]. Such angiogenesis inhibitors that target the VEGF-A$_{165}$/VEGFR-2/NRP-1 complex constitute a wide variety of compounds, including anti-VEGF or anti-VEGFR monoclonal antibodies [26–28], VEGFR-binding peptides and proteins [23,29,30], small molecular inhibitors of receptor tyrosine kinases of VEGF receptors [22,31–33], and various NRP-1-targeting substances such as peptides and peptidomimetics [8,34–46]. A significant achievement was the identification (by a mutated phage library screening) of a heptapeptide Ala-Thr-Trp-Leu-Pro-Pro-Arg (A7R), which selectively inhibits VEGF$_{165}$ binding to NRP-1 and decreases breast cancer angiogenesis and growth in vivo [35,47]. Further studies of the shortest active fragment of A7R led to a more elaborate branched peptidomimetic, Lys(hArg)-Dab-Pro-Arg, which was a stronger inhibitor of VEGF-A$_{165}$ binding with NRP-1, as determined by an in vitro ELISA assay, and was more stable in human serum compared to A7R [43].

At the same time, angiogenesis inhibitors labeled with diagnostic radionuclides (emitters of gamma or beta plus radiation) or therapeutic radionuclides (emitters of Auger electrons and alpha or beta minus radiation) can serve as diagnostic or therapeutic radiopharmaceuticals, respectively. The diagnostic methods of nuclear medicine can detect diseases at an early stage, much earlier than the accompanying morphological changes that could be detected by classical medicinal diagnosis. Such early and apposite diagnoses strongly promote the effectiveness of consecutive therapy. Importantly, radiocompounds designed from these compounds must maintain their inhibitory activity despite modifications to their chemical structure, such as appending a chelator.

In recent years, targeting overexpressed receptors on tumor cells with radiolabeled peptides has become very important in anticancer therapy [48], so we decided to investigate two novel radioconjugates based on VEGF-A$_{165}$/NRP-1 inhibitors: the A7R peptide and Lys(hArg)-Dab-Pro-Arg peptidomimetic.

The aim of the presented research was the design and synthesis of novel radioconjugates as well as physicochemical characterization of the obtained radiocompounds in terms of the requirements for receptor radiopharmaceuticals.

2. Materials and Methods

2.1. Materials

Unless otherwise specified, reagents and solvents were obtained from commercial sources and used without further purification. Fmoc-Arg(Pbf)-Wang resin was obtained from Activotec (Cambridge, UK). Amino acids and coupling reagents were purchased from Iris Biotech (Marktredwitz, Germany). DOTA-tris(tBu)-NHS was purchased from CheMatech (Dijon, France). Pooled human serum (HS) was obtained from Innovative Research (Novi, MI, USA).

Ga-68 radionuclide (emitter β^+, $t_{1/2}$ = 67.7 min, $E_{\beta max}$ = 1.92 MeV) in the form of [^{68}Ga]GaCl$_3$ in 0.1 M HCl was obtained from a ^{68}Ge/^{68}Ga generator (Eckert & Ziegler, Germany). Lu-177 radionuclide (emitter β^- (76%), $t_{1/2}$ = 6.65 d, $E_{\beta max}$ = 0.497 MeV) in the form of [^{177}Lu]LuCl$_3$ in 0.04 M HCl was purchased from National Centre for Nuclear Research Radioisotope Centre POLATOM, Świerk-Otwock, Poland, at a specific activity $\geq$ 370 GBq/mg Lu.

Conjugate analyses were performed on a KNAUER RP-HPLC on an analytical Eurospher-100-C-18 column (5 μm, 250 × 4.6 mm). Radioconjugate analyses were performed on a Shimadzu RP-HPLC on a semi-preparative Phenomenex Jupiter Proteo 90Å column (4 μm, 250 × 10 mm) with a Jupiter Proteo precolumn (20 × 2.1 mm) and on an analytical Phenomenex Jupiter 4u Proteo 90Å column (4 μm, 250 × 4.6 mm).

Deionized water was prepared in a Hydrolab water purification system (Hydrolab, Straszyn, Poland).

2.2. Methods

2.2.1. Analytical Methods

Conjugates **1** and **2** (compounds with a DOTA chelator) were analyzed by reverse-phase high-pressure liquid chromatography (RP-HPLC) in System 1 or 2.

System 1: RP-HPLC analytical Eurospher-100-C-18 column, 5 μm, 250 × 4.6 mm, solvent A: water with 0.1% trifluoroacetic acid (TFA, *v/v*), solvent B: acetonitrile/water (80:20, *v/v*) with 0.1% TFA (*v/v*), UV/Vis detection at 220 nm, gradient elution: 0–20 min 20 to 70% B, flow 1 mL/min.

System 1a: RP-HPLC semi-preparative Nucleosil-300-C18 column, 5 μm, 250 × 8 mm, solvent A: water with 0.1% trifluoroacetic acid (TFA, *v/v*), solvent B: acetonitrile/water (80:20, *v/v*) with 0.1% TFA (*v/v*), UV/Vis detection at 220 nm, gradient elution: 0–5 min 8% B, 5–15 min 8 to 18% B, 15–25 min 18% B, 25–35 min 18 to 35% B, 35–55 min 35% B, 55–60 min 35 to 40% B, 60–65 min 40 to 100% B, flow 2 mL/min.

System 2: RP-HPLC analytical Eurospher-100-C-18 column, 5 μm, 250 × 4.6 mm, solvent A: water with 0.1% TFA (*v/v*), solvent B: acetonitrile/water (80:20, *v/v*) with 0.1% TFA (*v/v*), UV/Vis detection at 220 nm, gradient elution: 0–20 min 5 to 60% B, flow 1 mL/min.

System 2a: RP-HPLC semi-preparative Nucleosil-300-C18 column, 5 μm, 250 × 8 mm, solvent A: water with 0.1% trifluoroacetic acid (TFA, *v/v*), solvent B: acetonitrile/water (80:20, *v/v*) with 0.1% TFA (*v/v*), UV/Vis detection at 220 nm, gradient elution: 0–15 min 5 to 15% B, 15–45 min 15% B, 45–55 min 15 to 100% B, flow 2 mL/min.

Analyses and purification of the radiopreparations and their cold reference compounds were performed in Systems 3 or 4 using the RP-HPLC method with gamma or UV/Vis detection, respectively. Radioactivity of the collected samples were measured using Wizard^2 2-Detector Gamma Counter (PerkinElmer) and/or Atomlab 500 Dose Calibrator (BIODEX). Electrospray ionization mass spectrometry analyses (ESI-MS) were performed to confirm the presence of the proper compounds.

System 3: RP-HPLC semi-preparative Phenomenex Jupiter Proteo 90Å column, 4 μm, 250 × 10 mm, with Jupiter Proteo precolumn, 20 × 2.1 mm, gamma or UV/VIS detection (220 nm), solvent A: acetonitrile with 0.1% TFA (*v/v*), solvent B: water with 0.1% TFA (*v/v*), gradient elution: 0–20 min 20 to 80% A, 20–30 min 80% A, 30–32 min 80 to 20% A, flow 2 mL/min.

System 4: RP-HPLC analytical Phenomenex Jupiter 4u Proteo 90Å column, 4 μm, 250 × 4.6 mm, gamma or UV/VIS detection (220 nm), solvent A: acetonitrile with 0.1% TFA (*v/v*), solvent B: water with 0.1% TFA (*v/v*), gradient elution: gradient elution: 0–20 min 1 to 50% A, 20–25 min 50 to 95% A, 25–31 min 95% A, 31–35 min 95 to 1% A. flow 1 mL/min.

2.2.2. Syntheses

Synthesis of conjugates **1** and **2**

The synthesis of conjugates DOTA-Ahx-A7R (**1**, Figure 1A) and Lys(hArg)-Dab(Ahx-DOTA)-Pro-Arg (**2**, Figure 1B), based on A7R (Figure 1A black) as a parent peptide and its shorter analogue Lys(hArg)-Dab-Pro-Arg (Figure 1B black), respectively, were carried out manually, on the preloaded Fmoc-Arg(Pbf)-Wang resin with a capacity of 0.32 mmol/g (0.48 mmol scale), following the Fmoc chemistry. Coupling of 3 eq. amino acids was done using 3 eq. DIC and 3 eq. HOBt in DMF (3 mL) [49]. Completion of coupling was checked using a Kaiser [50] or chloranil test [51]. Fmoc deprotection step was done using 30% piperidine in DMF. Guanylation reaction was performed for 4 days using di-Boc-S-methylisothiourea (3 eq. in 3 mL DCM) [52]. The Alloc deprotection step was done using tetrakis(triphenylphosphine)palladium(0) (0.06 mmol; 0.25 eq.) in the presence of 24 eq. PhSiH$_3$ (5.76 mmol) in DCM [53]. The coupling of the chelator was performed using the active ester method with 1 eq. DOTA-tris(tBu)-NHS and 3 eq. Et$_3$N for about 20 h.
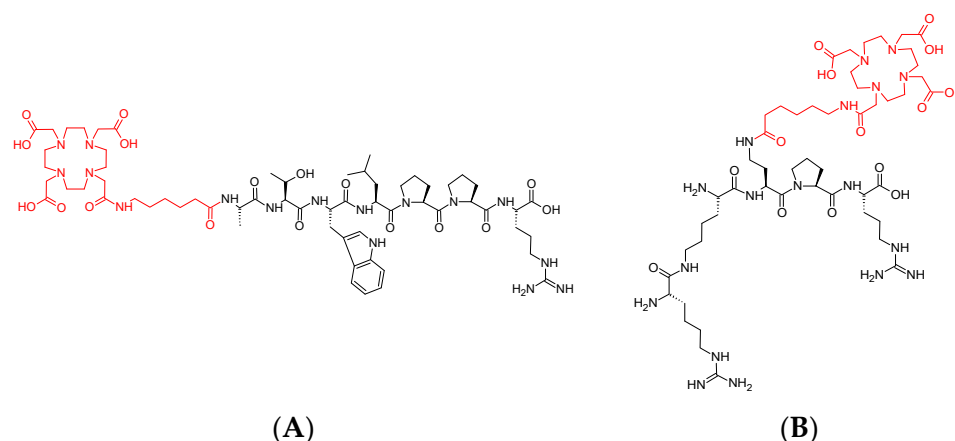
Figure 1. Chemical structure of molecules: (**A**) DOTA-Ahx-A7R (conjugate **1**); (**B**) Lys(hArg)-Dab(Ahx-DOTA)-Pro-Arg (conjugate **2**). The DOTA chelator and Ahx linker that were attached to the parent compounds (in black) are shown in red.

The cleavage of the final conjugates were performed using the mixture of TFA:PhOH:H_2O:TIPS (88:5:5:2, *v/v/v/v*) for 2 h. Crude conjugates were precipitated by a dropwise addition into a cold diethyl ether, and then were purified using semi-preparative KNAUER RP-HPLC in System 1a for conjugate **1** and System 2a for conjugate **2**. Purified conjugates were analyzed by mass spectrometry method (ESI-MS).

Preparation of [^{68}Ga]Ga-DOTA-Ahx-A7R (^{68}Ga-1) and [^{68}Ga]Lys(hArg)-Dab(Ahx-DOTA-Ga)-Pro-Arg (^{68}Ga-2) radioconjugates

[^{68}Ga]Ga-DOTA-Ahx-A7R (**^{68}Ga-1**) and [^{68}Ga]Lys(hArg)-Dab(Ahx-DOTA-Ga)-Pro-Arg (**^{68}Ga-2**) radioconjugates were synthesized according to the following procedure: into a vial containing about 10–20 nmol of lyophilized conjugate **1** or conjugate **2,** we added 300–400 μL of 0.2 M acetate buffer (pH 4.5), and 200–300 μL of the [^{68}Ga]GaCl$_3$ (10–30 MBq) solution from the ^{68}Ge/^{68}Ga generator. The reaction mixture at pH 3.0 was heated for 10 min at 95 °C. The resulting radioconjugates were then purified by RP-HPLC in System 3 with gamma detection for radioconjugate **^{68}Ga-1** (RCY 93.3 ± 0.3%, *n* = 4, molar activity 1.2 MBq/nmol, pH 3.0) and in System 4 with gamma detection for radioconjugate **^{68}Ga-2** (RCY 91.5 ± 0.8%, *n* = 4, molar activity 1.2 MBq/nmol, pH 3.0). Pure fractions of **^{68}Ga-1** and **^{68}Ga-2** radioconjugates were evaporated under N_2 and dissolved on PBS.

Preparation of [^{177}Lu]Lu-DOTA-Ahx-A7R (^{177}Lu-1) and [^{177}Lu]Lys(hArg)-Dab(Ahx-DOTA-Lu)-Pro-Arg (^{177}Lu-2) radioconjugates

[^{177}Lu]Lu-DOTA-Ahx-A7R (**^{177}Lu-1**) and [^{177}Lu]Lys(hArg)-Dab(Ahx-DOTA-Lu)-Pro-Arg (**^{177}Lu-2**) radioconjugates were synthesized according to the following procedure: into a vial containing about 2.5–20 nmol of lyophilized conjugate **1** or conjugate **2,** we added 200–300 μL of 0.2 M acetate buffer (pH 4.5), 150–200 μL H_2O, and 5–15 μL of the [^{177}Lu]LuCl$_3$ (1–15 MBq) solution. In some cases, we also added 0.5–2.0 μL 0.1 M HCl to obtain a desired pH. The reaction mixture at pH 4.5 was heated for 10 min at 95 °C. The resulting conjugates were then purified by RP-HPLC in System 3 with gamma detection for radioconjugate **^{177}Lu-1** (RCY 95.5 ± 1.2%, *n* = 4, molar activity 0.3 MBq/nmol, pH 4.5) and in System 4 with gamma detection for radioconjugate **^{177}Lu-2** (RCY 96.2 ± 2.6%, *n* = 4, molar activity 0.3 MBq/nmol, pH 4.5). Pure fractions of **^{177}Lu-1** and **^{177}Lu-2** radioconjugates were evaporated under N_2 and dissolved on PBS.

All radioconjugates were purified before the use in further experiments, namely, the lipophilicity and stability studies.

Preparation of cold reference compounds Ga/Lu-DOTA-Ahx-A7R (Ga/Lu-1) and Lys(hArg)-Dab(Ahx-DOTA-Ga/Lu)-Pro-Arg (Ga/Lu-2)

To verify the identity of the **^{68}Ga-1**, **^{177}Lu-1**, **^{68}Ga-2**, and **^{177}Lu-2** radioconjugates, the analogues with stable gallium and lutetium isotopes under the same reaction conditions

were synthesized and analyzed by the RP-HPLC method (System 3 or 4 with UV/Vis detection) and ESI-MS methods.

Ga-DOTA-Ahx-A7R (**Ga-1**) and Lys(hArg)-Dab(Ahx-DOTA-Ga)-Pro-Arg (**Ga-2**) cold reference compounds were synthesized according to the following procedure: into a vial containing approximately 70 nmol of conjugate **1** or **2** dissolved in 300 µL of 0.2 M acetate buffer (pH 4.5), we added the 60 µL of 1.34 mg/mL GaCl$_3$ solution in 0.065 M HCl. The reaction mixture at pH 4.0 was heated for 10 min at 95 °C. The reaction progress was checked by RP-HPLC in System 3 for **Ga-1** and in System 4 for **Ga-2**.

Lu-DOTA-Ahx-A7R (**Lu-1**) and Lys(hArg)-Dab(Ahx-DOTA-Lu)-Pro-Arg (**Lu-2**) cold reference compounds were synthesized according to the following procedure: to a vial containing approximately 70 nmol of conjugate **1** or **2** dissolved in 600 µL of 0.2 M acetate buffer (pH 4.5), we added the 3.5 µL of concentrated LuCl$_3$ solution in 14 M HCl. The reaction mixture at pH 4.0 was heated for 10 min at 95 °C. The reaction progress was checked by RP-HPLC in System 3 for **Lu-1** and in System 4 for **Lu-2**.

2.2.3. Physicochemical Properties Study of the Radioconjugates

All studies of the physicochemical properties of the synthesized radiopreparations were carried out using radioconjugates previously isolated from the reaction mixture.

Radioconjugates lipophilicity test

The lipophilicity (L) of tested radiocompounds, defined as the decimal logarithm (logP) of the partition coefficient (P) of the compound between the two immiscible phases, was determined in the system PBS solution (aqueous phase, polar phase, pH 7.4) and *n*-octanol (organic, non-polar phase) according to the following formula:

$$L = \log P = \log \frac{A_o}{A_w}$$

where A_o—organic phase radioactivity; A_w—aqueous phase radioactivity.

Radioactivity of both phases, resulting from the concentration of the tested radiocompound in each of them, was determined by measuring the gamma radiation with a Wizard counter in three independent experiments.

Before starting the research, both liquid phases were saturated with each other to avoid errors resulting from the mutual solubility of both liquids. The partition coefficient (P) result is shown as the mean ± SD. After the end of the experiment, we performed RP-HPLC analysis of the aqueous phase to confirm the tested radioconjugate remained intact during the experiment.

Radioconjugates stability tests

In accordance with requirements for potentially novel radiopharmaceuticals, we tested newly designed radiopreparations for their stability in solutions that act as human body fluids and also in human serum [54,55].

Stability studies in PBS buffer, cysteine and histidine

Stability studies in PBS buffer were performed in order to investigate the possible influence of buffer components on the radiocompound decomposition process. We isolated ^{68}**Ga-1**, ^{177}**Lu-1**, ^{68}**Ga-2**, and ^{177}**Lu-2** radioconjugates from the reaction mixture and incubated each in PBS buffer. After about 3 h, we analyzed aliquots by RP-HPLC in System 3 with gamma detection for ^{68}**Ga-1** and ^{177}**Lu-1** and in System 4 with gamma detection for ^{68}**Ga-2** and ^{177}**Lu-2**.

Stability studies of the isolated from the reaction mixture ^{68}**Ga-1**, ^{177}**Lu-1**, ^{68}**Ga-2,** and ^{177}**Lu-2** radioconjugates in solutions containing excess amounts of strongly competing natural ligands with chemically reactive groups, e.g., -NH$_2$, -SH, and -COOH (the so-called challenge experiments). For this purpose, each radioconjugate was incubated at 37 °C in 1 mM cysteine (Cys) or histidine (His) solutions in PBS buffer (the ligand concentration was about 1000 times higher than the concentration of tested radioconjugate). After the specified incubation time, which was up to 4 h for the ^{68}Ga-radiocompounds and up to 6 days for the ^{177}Lu-radiocompounds, we analyzed solutions by RP-HPLC in System 3

with gamma detection for ^{68}**Ga-1** and ^{177}**Lu-1** and in System 4 with gamma detection for ^{68}**Ga-2** and ^{177}**Lu-2**.

Stability studies in human serum

Stability studies of the ^{68}**Ga-1**, ^{177}**Lu-1**, ^{68}**Ga-2**, and ^{177}**Lu-2** radioconjugates in human serum (HS) were performed according to the following procedure: into a vial containing 900 μL of HS we added 100 μL of the tested radioconjugate and incubated the mixture at 37 °C. After the specified incubation times (10 min–4.5 h for ^{68}Ga-radiocompounds and 10 min–4 days for ^{177}Lu-radiocompounds), we withdrew the aliquots, mixed with ethanol to precipitate the proteins, and centrifuged (14,000 rpm, 5–15 min) to separate the protein compounds from the supernatant. The gamma radioactivity of the obtained precipitate and supernatant was then measured using a Wizard detector. Using the formula below, the amount of radioconjugate remaining in the supernatant (and also bound by serum protein components) was calculated.

$$\frac{\sum \text{ liquid phase radioactivity}}{\sum \text{ liquid phase radioactivity} + \sum \text{ percipitate radioactivity}} \times 100\%$$

We also analyzed the supernatant at each time by RP-HPLC in System 3 with gamma detection for ^{68}**Ga-1** and ^{177}**Lu-1** and System 4 with gamma detection for ^{68}**Ga-2** and ^{177}**Lu-2** to check whether the studied radiocompound remained unchanged during the experiment.

3. Results

3.1. Syntheses of Conjugates *1* and *2*

The synthesis of conjugates **1** and **2** (Scheme 1) was carried out by Solid Phase Peptide Synthesis (SPPS) on the preloaded Fmoc-Arg(Pbf)-Wang resin following the Fmoc chemistry according to the standard coupling DIC/HOBt protocol. In the case of synthesis of conjugate **1**, after building a linear peptide on the resin and coupling of the Ahx spacer, the chelator DOTA was attached by the active ester method using DOTA-tris(tBu)-NHS.

The synthesis of conjugate **2** required a few additional steps, as shown in Scheme 1. After the synthesis of fully protected, linear tripeptide (Fmoc-Dab(Alloc)-Pro-Arg(Pbf)-Wang), we attached the N-terminal lysine using Boc-Lys(Fmoc), which enabled the attachment of another Boc-Lys(Fmoc) to the side chain after removal of the Fmoc group from the epsilon amino group. After Fmoc deprotection of the epsilon amino group of the second lysine, we carried out the guanylation reaction for 4 days to lead to hArg creation using di-Boc-S-methylisothiourea, until the Kaiser test was negative. Next, after Alloc deprotection of the amino group of the side chain of the Dab residue, we coupled Fmoc-Ahx. Following the coupling sequence, Fmoc deprotection was performed as the next step, and then the DOTA chelator was attached by the active ester method using DOTA-tris(tBu)-NHS. The cleavage of the synthetized compounds from the resin was performed using the TFA:PhOH:H$_2$O:TIPS mixture simultaneously removing all Boc protections. We purified the crude compounds by RP-HPLC and analyzed by ESI-MS (Table 1).
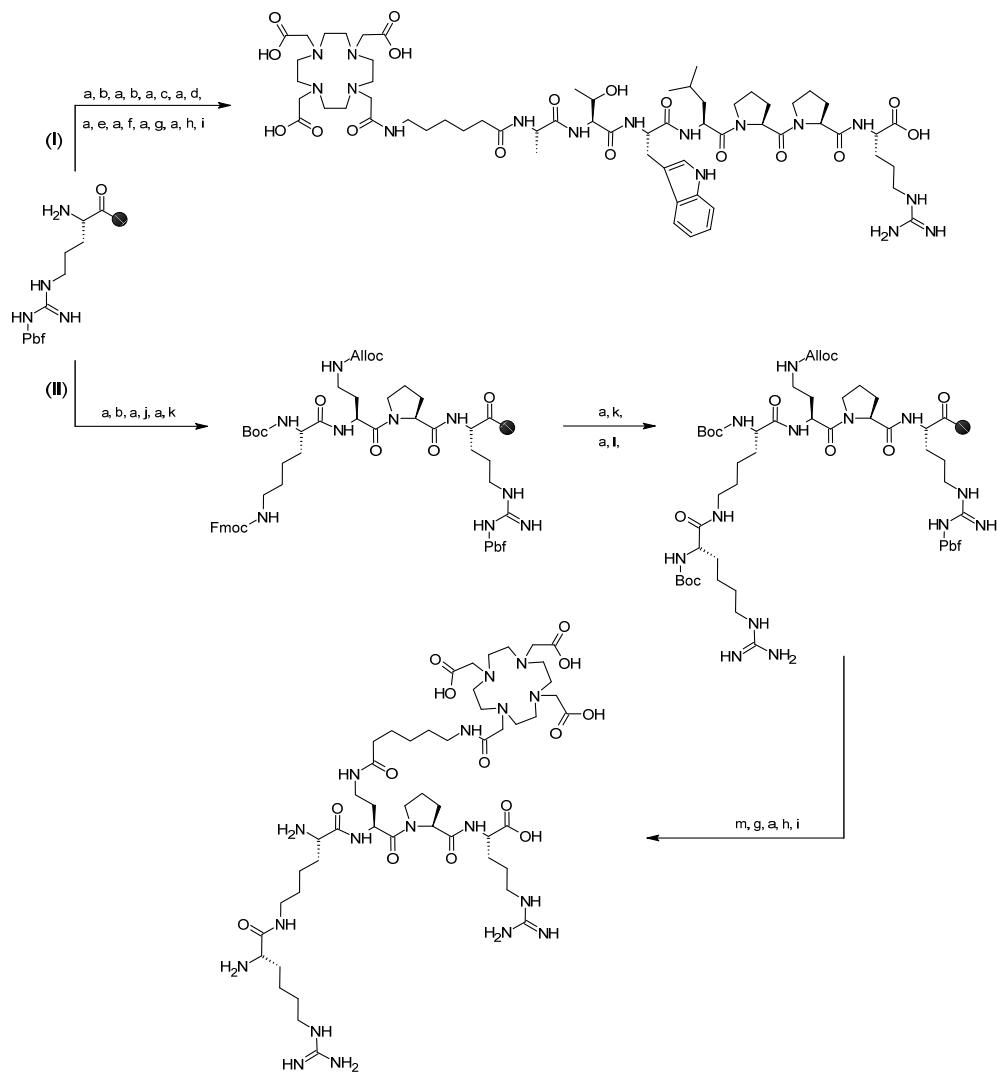
Scheme 1. Synthesis strategy of conjugate **1** (path I) and **2** (path II) by SPPS method. a—30% piperidine in DMF; b—Fmoc-Pro-OH:DIC:HOBt; c—Fmoc-Leu-OH:DIC:HOBt; d—Fmoc-Trp(Boc)-OH:DIC:HOBt; e—Fmoc-Thr(tBu)-OH:DIC:HOBt; f—Fmoc-Ala-OH:DIC:HOBt; g—Fmoc-Ahx-OH:DIC:HOBt; h—DOTA-tris(tBu)-NHS:triethylamine; i—TFA/PhOH/H$_2$O/TIPS; j—Fmoc-L-Dab(Alloc)-OH:DIC:HOBt; k—Boc-Lys(Fmoc)-OH:DIC:HOBt; l—di-Boc-S-methylisothiourea:n-butylamine:DCM; m—phenylsilane:tetrakis(triphenylphosphine)-palladium:DCM.

Table 1. Results of the ESI-MS analyses of synthesized conjugates **1** and **2**.

Conjugate	R$_T$ (min) (RP-HPLC System)	Signal Found (m/z)	Signal Calculated (m/z)
1	10.9 (1)	[M+3H]$^{3+}$: 447.5	[M+3H]$^{3+}$: 447.0
		[M+2H]$^{2+}$: 670.7	M+2H]$^{2+}$: 670.0
		[M−2H]$^{2-}$: 668.6	[M−2H]$^{2-}$:668.0
		[M−H]$^-$: 1337.9	[M−H]$^-$: 1337.9
2	9.3 (2)	[M+4H]$^{4+}$: 293.2	[M+4H]$^{4+}$: 293.0
		[M+3H]$^{3+}$: 390.6	[M+3H]$^{3+}$: 390.3
		[M+2H]$^{2+}$: 585.4	[M+2H]$^{2+}$: 585.0
		[M−H]$^-$: 1167.7	[M−H]$^-$: 1167.0

3.2. Syntheses of Radioconjugates

All obtained radiocompounds were formed with high radiochemical yield (>90% for [68]Ga-1 and ^{68}Ga-2, and >95% for [177]Lu-1 and [177]Lu-2) and high radiochemical purity (>90%). The chemical formulas of the ^{68}Ga-1, ^{177}Lu-1, ^{68}Ga-2, and [177]Lu-2 radioconjugates as well as the RP-HPLC radiochromatograms of the labeling reaction mixtures are presented in Figure 2. The statistical data of the radiochemical yield (RCY) and radiochemical purity (RCP) (presented as the mean ± SD, n = the number of repetitions) of the obtained ^{68}Ga-1, ^{177}Lu-1, ^{68}Ga-2, and [177]Lu-2 radioconjugates are presented in Table 2.
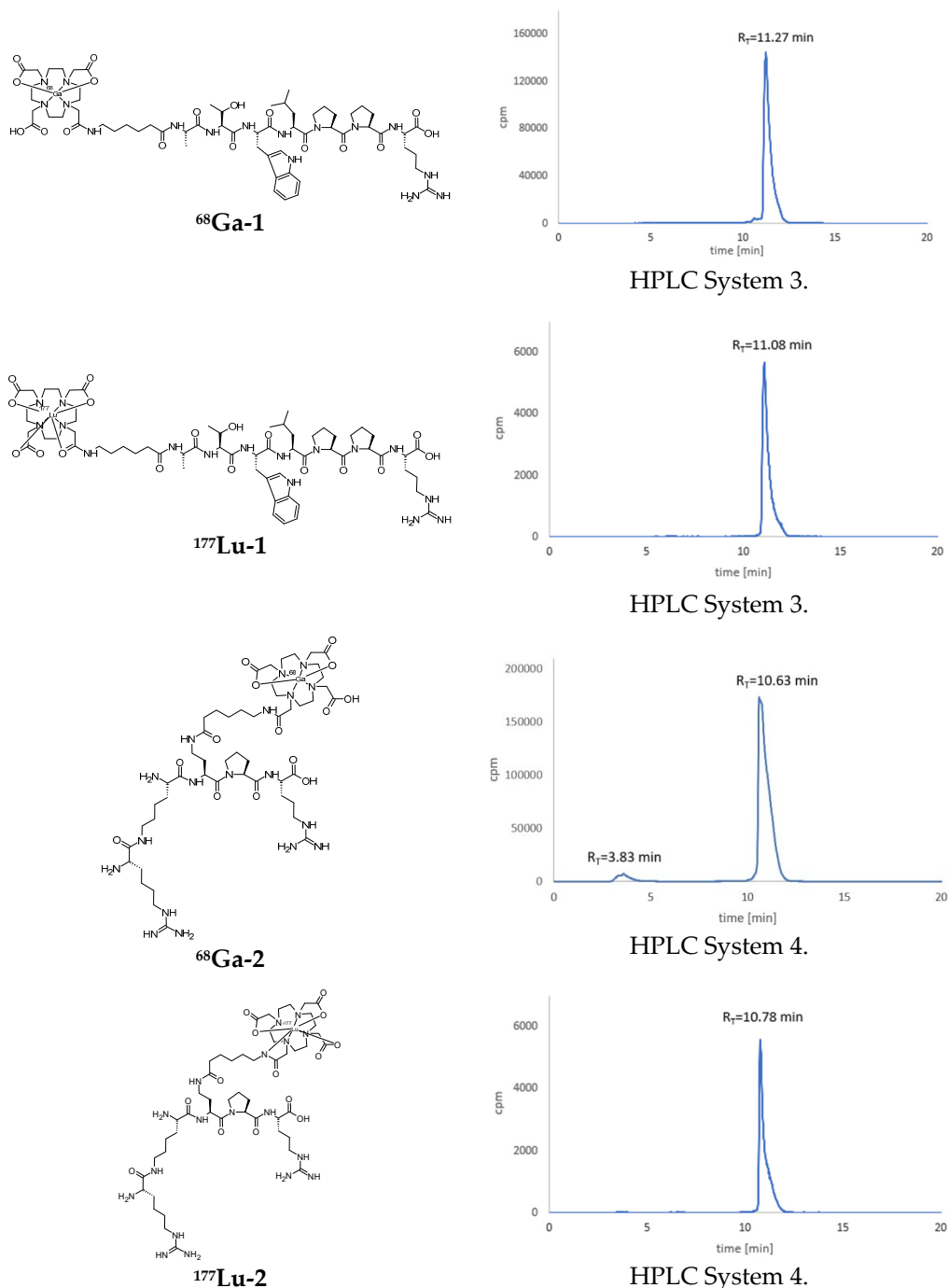
Figure 2. The chemical structures (**left**) and RP-HPLC radiochromatograms (**right**) of the ^{68}Ga-1, ^{177}Lu-1, ^{68}Ga-2, and [177]Lu-2 radioconjugates.

Table 2. Results of radiochemical yield and radiochemical purity of the synthesized ⁶⁸**Ga-1**, ¹⁷⁷**Lu-1**, ⁶⁸**Ga-2**, and ¹⁷⁷**Lu-2** radioconjugates.

Radioconjugate	RCY ± SD, *n* = 4 (%)	RCP ± SD, *n* = 4 (%)
^{68}**Ga-1**	93.3 ± 0.3	97.1 ± 0.9
^{177}**Lu-1**	95.5 ± 1.2	99.8 ± 0.9
^{68}**Ga-2**	91.5 ± 0.8	93.4 ± 0.3
^{177}**Lu-2**	96.2 ± 2.6	99.3 ± 1.9

3.3. Synthesis of Cold References Compounds

RP-HPLC analyses of the reaction mixtures of the cold reference compounds are presented in Figure 3. The compounds characterized with R_T values as 10.83 min, 10.75 min, 10.46 min, and 10.35 min were isolated from the reaction mixture and identified by ESI-MS as Ga-DOTA-Ahx-A7R (**Ga-1**), Lu-DOTA-Ahx-A7R (**Lu-1**), Lys(hArg)-Dab(Ahx-DOTA-Ga)-Pro-Arg (**Ga-2**), and Lys(hArg)-Dab(Ahx-DOTA-Lu)-Pro-Arg (**Lu-2**), respectively. The R_T values of these reference compounds coincided with the corresponding retention times of the appropriate radiocompounds (⁶⁸**Ga-1**, ¹⁷⁷**Lu-1**, ⁶⁸**Ga-2**, and ¹⁷⁷**Lu-2**; Figure 3), which confirmed the stability of both the A7R and Lys(hArg)-Dab-Pro-Arg molecules under these synthesis conditions and confirmed that we obtained the desired radiocompounds.
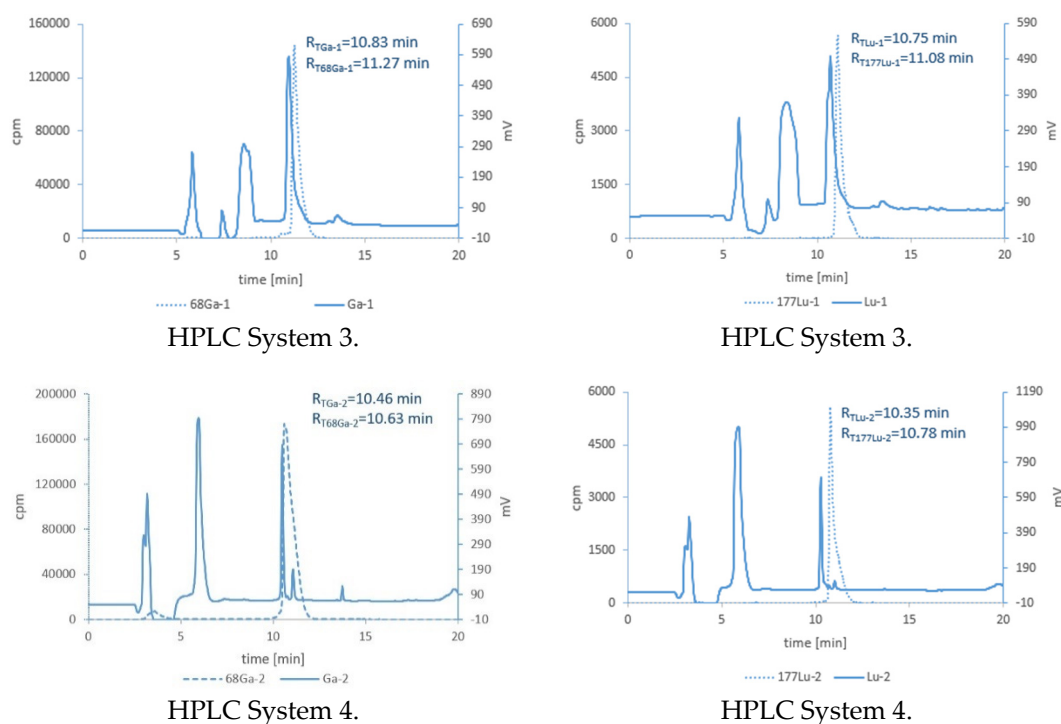
Figure 3. RP-HPLC chromatograms of the reaction mixtures of the cold reference compounds **Ga-1**, **Lu-1**, **Ga-2**, and **Lu-2**—solid lines—and their corresponding radioconjugates ⁶⁸**Ga-1**, ¹⁷⁷**Lu-1**, ⁶⁸**Ga-2**, and ¹⁷⁷**Lu-2**—dotted lines.

The results of ESI-MS analyses confirming the cold reference compounds were obtained are shown in Table 3.

Table 3. Results of ESI-MS analyses of the synthesized cold reference compounds **Ga-1**, **Lu-1**, **Ga-2**, **Lu-2**.

Compound	R_T (min) (RP-HPLC System)	Signal Found (m/z)	Signal Calculated (m/z)
Ga-1	10.83 (3)	$[M]^+$: 1405.60 and 1407.61	$[M]^+$: 1405.64 and 1407.64
Lu-1	10.75 (3)	$[M+H]^+$: 1511.63	$[M+H]^+$: 1511.66
Ga-2	10.46 (4)	$[M]^+$: 1235.60 and 1237.63	$[M]^+$: 1235.62 and 1237.62
Lu-2	10.35 (4)	$[M+H]^+$: 1341.59	$[M+H]^+$: 1341.62

3.4. Lipophilicity Studies

Lipophilicity is one of the most important physicochemical parameters affecting the absorption, distribution, metabolism, and excretion of drug molecules in the organism, the so-called ADME profile [56–59]. Preparations characterized by high lipophilicity show a high affinity for fats and a low affinity for water; they are also able to effectively penetrate cell membranes. From the point of view of pharmacology, lipophilicity is an important prognostic factor for drugs and other medical preparations to predict toxic activity and to characterize biological activity, the ability to accumulate in organisms, and the metabolism of substances [60–65]. The lipophilicity values obtained for tested radioconjugates ^{68}Ga-1, ^{177}Lu-1, ^{68}Ga-2, and [177]Lu-2 (presented as the mean $\pm$ SD) are shown in Table 4. The main reason for the low lipophilicity value is that the tested radiocompounds are based on peptides and peptidomimetics, which are usually characterized by a low lipophilicity value. Moreover, conjugation of the macrocyclic DOTA chelator with the biomolecule also results in a lower lipophilicity value of the conjugate compared to the lipophilicity of the biomolecule itself.

Table 4. R_T and logP values of the tested radioconjugates.

Radiocompound	RP-HPLC System	R_T (min)	logP $\pm$ SD
[68]Ga-1	3	11.27	-3.92 ± 0.03
[177]Lu-1	3	11.08	-3.40 ± 0.14
[68]Ga-2	4	10.63	-4.57 ± 0.05
[177]Lu-2	4	10.78	-3.75 ± 0.08

Radiochromatograms of the aqueous phases after the lipophilicity tests of the radio-preparations showed, in all cases, single peaks at R_T values that corresponded to the tested radiocompounds, which proves the stability of the radiopreparations during the experiment.

3.5. Stability Studies of Radioconjugates in PBS Buffer, Cysteine and Histidine

Stability tests of all radioconjugates incubated in PBS solution for about 3 h showed no decomposition of radioconjugates. In all the RP-HPLC radiochromatograms only single peaks were recorded, with R_T values that corresponded to the appropriate radioconjugate, which confirms the stability of radioconjugates under such conditions.

3.6. Stability Tests for [68]Ga-1 and [68]Ga-2 Radioconjugates

Stability tests of the [68]Ga-1 radioconjugate in the Cys (Figure 4 left) and His (Figure 4 right) solutions showed satisfactory stability in the period of about 3 h, corresponding to the three half-lives of the radionuclide gallium-68. In the RP-HPLC radiochromatograms recorded after 3 h, we observed only traces of the products of radioconjugate decomposition (Figure 4).
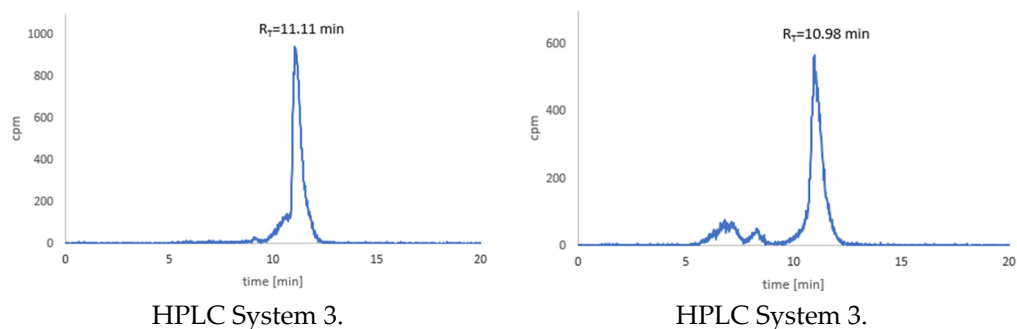
HPLC System 3.   HPLC System 3.

Figure 4. RP-HPLC radiochromatograms (System 3) of the stability studies of the ^{68}**Ga-1** radioconjugate in Cys (**left**, RCP 95.2 ± 1.5%, *n* = 3) and His (**right**, RCP 76.2 ± 2.7%, *n* = 3) solutions recorded after 3.5 h of incubation.

Similarly, stability studies of the ^{68}**Ga-2** radioconjugate in Cys (Figure 5 left) and His (Figure 5 right) solutions carried out over the same time interval demonstrated the complete stability of the radioconjugate.
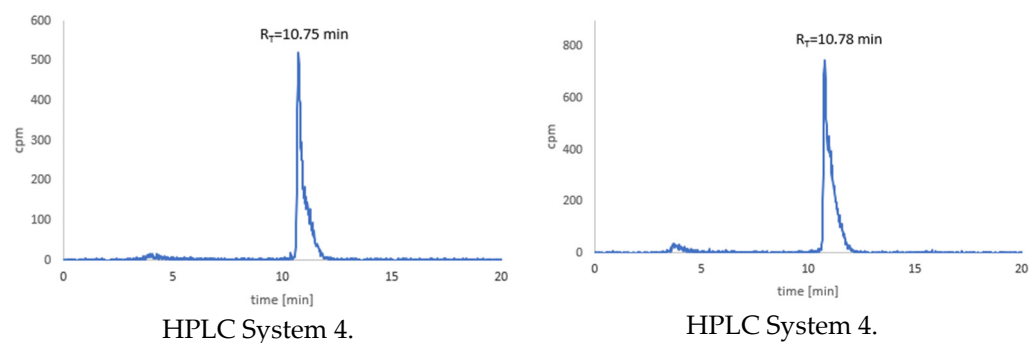

HPLC System 4.   HPLC System 4.

Figure 5. RP-HPLC radiochromatograms (System 4) of the stability studies of the ^{68}**Ga-2** radioconjugate in Cys (**left**, RCP 98.1 ± 1.2%, *n* = 3) and His (**right**, RCP 95.3 ± 2.0%, *n* = 3) solutions recorded after 3.5 h of incubation.

3.7. Stability Tests for ^{177}Lu-1 and ^{177}Lu-2 Radioconjugates

Stability studies of the radioconjugates containing lutetium-177 radionuclide in Cys and His solutions were carried out in the period of about 6 days, corresponding to the one half-live of the radionuclide lutetium-177. Incubation of the ^{177}**Lu-1** radioconjugate in Cys and His solutions for a longer period, more than 4 days, showed slow degradation of this radiopreparation in both solutions (Figure 6). The radioconjugate was completely stable for 1 day, but after 6 days, traces of the products of radioconjugate decomposition were already visible, and the degradation of the radioconjugate was noticeably higher during incubation in the His solution (Figure 6 right).

In contrast, the ^{177}**Lu-2** radioconjugate proved to be completely stable in both solutions throughout the incubation period (Figure 7).
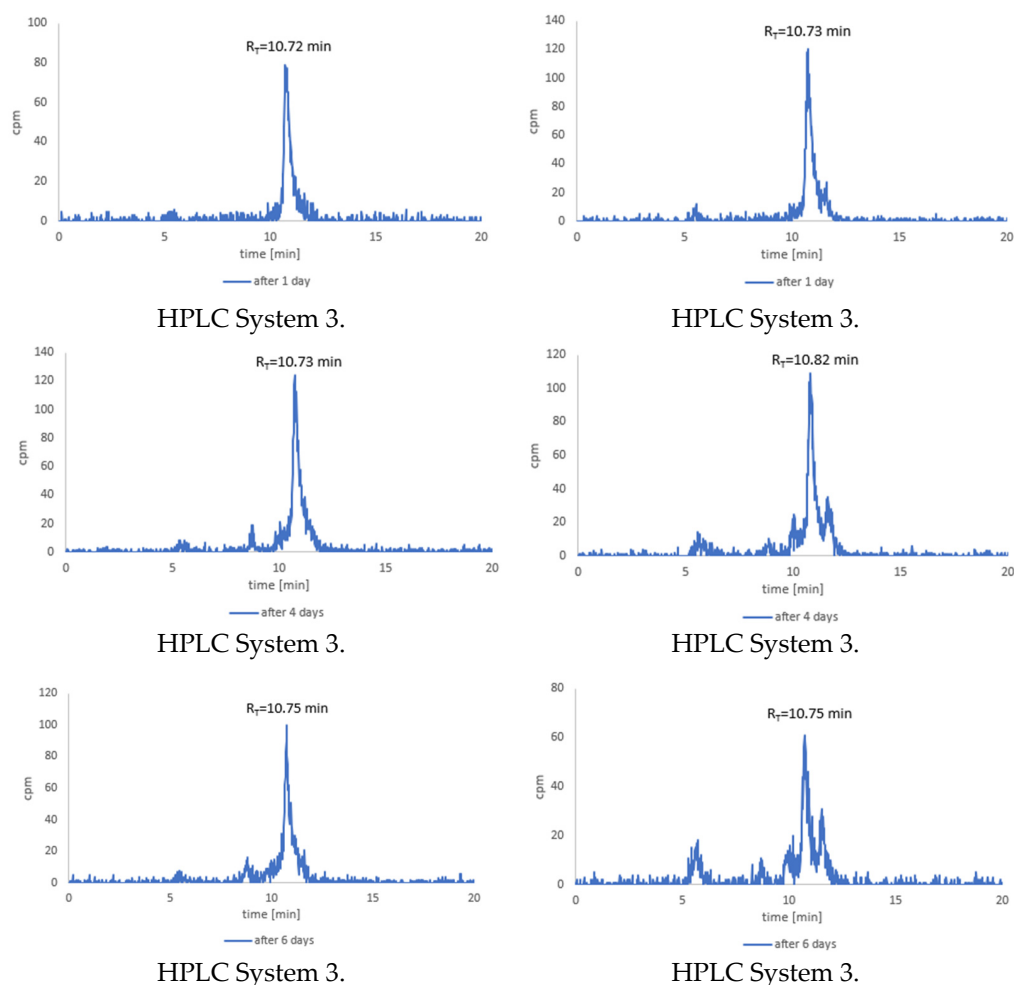
Figure 6. RP-HPLC radiochromatograms (System 3) of the stability studies of the [177]Lu-1 radioconjugate in Cys (**left**, after 1 day RCP 98.2 ± 2.5%, *n* = 3; after 4 days RCP 94.5 ± 3.0, *n* = 3; after 6 days RCP 93.0 ± 3.6%, *n* = 3) and His (**right**, after 1 day RCP 95.6 ± 2.5%, *n* = 3; after 4 days RCP 82.2 ± 3.2%, *n* = 3; after 6 days RCP 64.5 ± 4.1%, *n* = 3) solutions recorded after different time intervals.

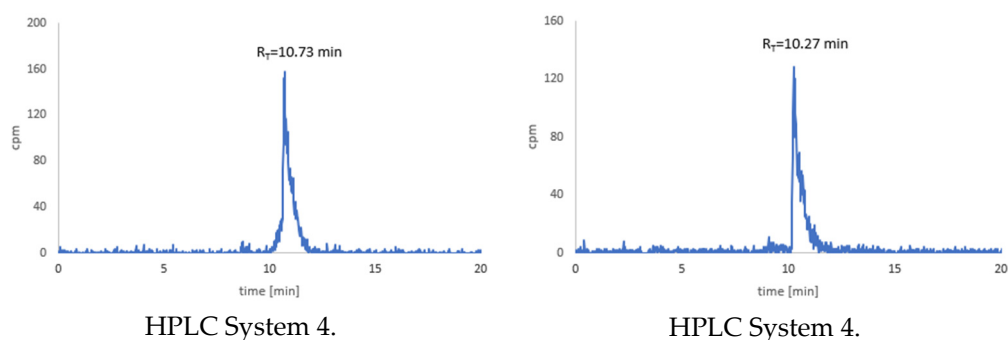**Figure 7.** RP-HPLC radiochromatograms (System 4) of the stability studies of the [177]Lu-2 radioconjugate in Cys (**left**, RCP 98.3 ± 2.5%, *n* = 3) and His (**right**, RCP 98.3 ± 2.8%, *n* = 3) solutions recorded after 6 days.

3.8. Stability Studies of Radioconjugates in Human Serum

Radiochromatograms illustrating the results of the stability tests of the ^{68}Ga-1, [177]Lu-1 and ^{68}Ga-2, [177]Lu-2 radioconjugates in human serum are shown in Figure 8. The statistical data of the radiochemical purity (presented as the mean ± SD, *n* = the number of repetitions)

of the obtained ^{68}**Ga-1**, ^{177}**Lu-1**, ^{68}**Ga-2**, and ^{177}**Lu-2** radioconjugates in the human serum stability tests are presented in Table 5.

HPLC System 3.   HPLC System 4.
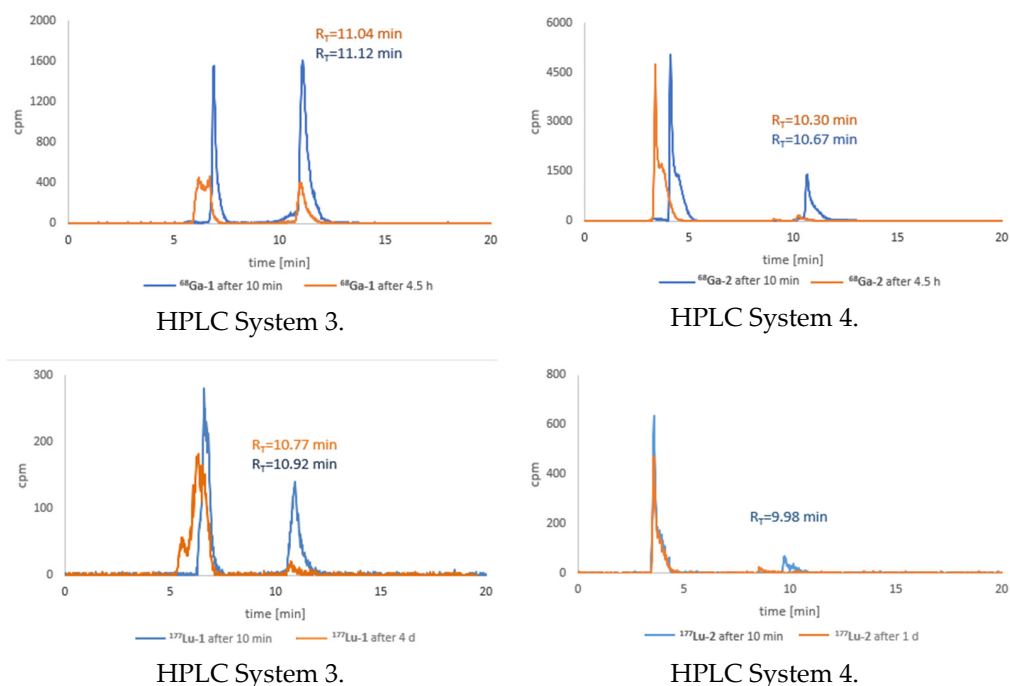
HPLC System 3.   HPLC System 4.

Figure 8. RP-HPLC radiochromatograms illustrating the results of the stability tests of the ^{68}**Ga-1** and ^{177}**Lu-1** (**left**, System 3) and ^{68}**Ga-2**, ^{177}**Lu-2** (**right**, System 4) radioconjugates in human serum recorded after different time intervals.

Table 5. Statistical data of the ^{68}**Ga-1**, ^{177}**Lu-1**, ^{68}**Ga-2**, and ^{177}**Lu-2** radioconjugates radiochemical purity corresponding to the radiochromatograms presented in Figure 8.

Radioconjugate	RCP $\pm$ SD, $n = 3$ (%)			
	after 10 min	**after 4.5 h**	**after 1 day**	**After 4 days**
^{68}**Ga-1**	65.3 $\pm$ 3.7	36.6 $\pm$ 1.4	n/a	n/a
^{68}**Ga-2**	27.7 $\pm$ 2.0	3.6 $\pm$ 0.2	n/a	n/a
^{177}**Lu-1**	39.2 $\pm$ 2.0	—	—	2.6 $\pm$ 0.2
^{177}**Lu-2**	13.8 $\pm$ 1.5	—	2.7 $\pm$ 0.1	—

As can be seen, all radioconjugates were unstable in HS due to biodegradation of the A7R peptide and Lys(hArg)-Dab-Pro-Arg peptidomimetic by endogenous enzymes. After 10 min of incubation, the radiochromatograms already showed additional peaks corresponding to the enzymatic degradation products. During incubation, the height of these additional peaks increased, and the peak heights corresponding to the tested radioconjugates decreased. After about 4 h in the case of the ^{68}**Ga-1** and ^{68}**Ga-2** radioconjugates and about 4 days in the case of the ^{177}**Lu-1** and ^{177}**Lu-2** radioconjugates, the peaks corresponding to the tested radiopreparations were often hardly visible, indicating almost complete biodegradation of the radioconjugates. Radioactivity measurements of the precipitated protein serum components and the supernatants indicated that, in the case of the ^{68}**Ga-1** and ^{177}**Lu-1** radioconjugates, about 15% of the radiocompounds was bound to the protein serum components. In the case of the ^{68}**Ga-2** and ^{177}**Lu-2** radioconjugates, about 28% of the radiocompounds was bound with protein serum components.

4. Discussion

The aim of the present study was to synthesize and to characterize the physicochemical properties of radiolabeled A7R peptide and Lys(hArg)-Dab-Pro-Arg peptidomimetic for potential application as diagnostic or therapeutic receptor radiopharmaceuticals. According to the literature data, the heptapeptide A7R is known to be an effective antagonist of the VEGF-A$_{165}$ binding with NRP-1 and to show in vivo anti-angiogenic properties [35], whereas the Lys(hArg)-Dab-Pro-Arg peptidomimetic is much more active (IC$_{50}$ = 0.2 μM) than the heptapeptide A7R (IC$_{50}$ = 5.9 μM [42]), with a stability half-life in human serum that is nearly 2 days [41,43]. To be able to synthesize radioconjugates, we attached a DOTA chelator to the initial compounds—A7R or its shorter analogue—via an Ahx linker.

All the designed radioconjugates were synthesized with high radiochemical yield and high radiochemical purity (Figure 2 right), and the methods for their synthesis were relatively simple and cheap. Identity of the radioconjugates was confirmed by ESI-MS analysis of their cold reference compounds.

All radioconjugates turned out to be highly hydrophilic compounds with logP values in the range of −3.40 to −4.57 (Table 4). Moreover, the radioconjugates with Ga-68 turned out to be visibly less lipophilic due to a free carboxyl group of the DOTA chelator. These values were much lower than those preferred for radiopharmaceuticals, in the ranges of 1 to 4 and 1.5 to 2.5, which are suitable for crossing the blood–tissue [66] and blood–brain barriers [67], respectively. However, the ability to cross the blood–tissue barrier is not a crucial parameter in this case due to the presence of VEGF$_{165}$ in the endothelium, the single layer of squamous endothelial cells that lines the interior surface of blood vessels, and its ability to interact directly with blood.

Radioconjugates ^{68}**Ga-1** and ^{68}**Ga-2** and radioconjugate ^{177}**Lu-2** were sufficiently stable in solutions acting as human body fluids, PBS buffer, and Cys or His solutions. However, the stability of the ^{177}**Lu-1** radioconjugate that contained therapeutic radionuclide Lu-177 and based on the A7R peptide turned out to be rather insufficient. After 6 days of incubation, which is just one half-life of the radionuclide Lu-177, the radioconjugate decomposition products were already visible (Figure 6). Because this is a potential therapeutic radiopharmaceutical containing radionuclide with a half-life of 6.65 days, such stability in these solutions is rather low.

Stability studies of the radioconjugates in human serum showed relatively rapid decomposition of all radiocompounds due to enzymatic biodegradation of A7R peptide and Lys(hArg)-Dab-Pro-Arg peptidomimetic (Figure 8). Comparing the RP-HPLC radiochromatograms recorded after a 10 min incubation, it is apparent that the radioconjugates ^{68}**Ga-2** and ^{177}**Lu-2** were more readily biodegraded in HS compared to the radioconjugates ^{68}**Ga-1** and ^{177}**Lu-1**. In the case of ^{177}**Lu-1** radiopreparation after 4 days of incubation, the radioconjugate was still visible in the sample, while in the case of ^{177}**Lu-2** after 1 day of incubation, only traces of radioconjugate were present in the sample. Moreover, during the incubation of ^{68}**Ga-1** and ^{177}**Lu-1** in HS, about 15% of the radiopreparations were bound to the serum peptide components, while in the case of radioconjugates ^{68}**Ga-2** and ^{177}**Lu-2**, almost twice as much, about 28%. This difference can be explained by the less-polar nature of the A7R (Ala^1-Thr^2-Trp^3-Leu^4-Pro^5-Pro^6-Arg^7-OH) peptide and the polar nature of the Lys^1(hArg)-Dab^2-Pro^3-Arg^4 peptidomimetic. The former compound had three reactive functional groups—the guanidine group of Arg^7, the amine group of Ala^1, and the carboxyl group of Arg—while the peptidomimetic had six reactive functional groups—the three amino groups of Lys^1, hArg, and Dab^2, the two guanidine groups of hArg and Arg^4, and one carboxyl group of Arg^4. These reactive groups, depending on the pH and under the influence of external conditions, can assume, respectively, positive or negative charges, and interact with the protein components of the human serum. Despite the fact that one amine group was used to attach the DOTA chelator via the Ahx linker in both conjugates, the radioconjugates produced by the labeling reactions of conjugate **1** and **2** should still differ in charge, polarity, and chemical reactivity because of differences in the physicochem-

ical properties of their parent compounds, the A7R peptide and Lys(hArg)-Dab-Pro-Arg peptidomimetic.

Based on the above data, it should be assessed that, unfortunately, radioconjugates [68]**Ga-2** and [177]**Lu-2** that were based on the more biologically active biomolecule, Lys(hArg)-Dab-Pro-Arg peptidomimetic, were less stable in HS than those based on the A7R peptide, [68]**Ga-1** and [177]**Lu-1**. Such a low stability of [68]**Ga-2** and [177]**Lu-2** was initially surprising because, according to the literature data, the determined half-life of the Lys(hArg)-Dab-Pro-Arg peptidomimetic in HS was nearly 2 days (41 h), and the period of its complete decomposition in HS estimated from the graph was over 4 days [43]. As determined from our experiments, the period of almost complete enzymatic biodegradation of radioconjugate [177]**Lu-2**, resulting from enzymatic biodegradation of the Lys(hArg)-Dab-Pro-Arg peptidomimetic, was less than 1 day. These two seemingly contradictory results were due to the different conditions of the stability studies. In the first case, the peptidomimetic concentration in the sample was 0.9 μmol/mL, which allowed us to detect the biodegradation using the UV/VIS detection [43]. In the second case, the peptidomimetic concentration was equal to the concentration of the radioconjugate and was incomparably lower, i.e., about 2 nmol/mL; experiments with such a low radioconjugate concentration were possible due to using gamma detection. Consequently, in the first case, the test was carried out with saturation of the enzymes present in HS sample, while in the second case, the amount of the peptidomimetic was much smaller than the amount of enzyme. Hence, in the first case, intact peptidomimetic was visible in the sample for about 4 days, while this period was only 1 day in the present study.

To conclude, our study showed that all radioconjugates obtained in the presented work were not sufficiently stable in HS, and so they unfortunately do not fully meet the requirements for radiopharmaceuticals. Nevertheless, the structure of the peptidomimetics can be modified easily, which makes it possible to design a new formulation that is more stable in HS. In the near future, we plan to modify them by using D-amino acids or replacing one or more peptide bonds with their bioisosteres (e.g., N-methyl peptide bond, or reduced bond -CH_2-NH-). For radiopreparations sufficiently stable in human serum and suitable for in vivo applications, we plan more advanced biological tests (using NRP-1 overexpressing cell lines) and finally tests on living organisms (a biodistribution study in mice or rats).

Abbreviations

A7R	Ala-Thr-Trp-Leu-Pro-Pro-Arg-OH peptide
ACN	Acetonitrile
ADME	Absorption, distribution, metabolism, and excretion
Ahx	6-aminohexanoic acid
Alloc	Allyloxycarbonyl group
A_o	Organic phase radioactivity
A_w	Aqueous phase radioactivity
Boc	Tert-butyloxycarbonyl group
COOH	Carboxyl group
Cys	Cysteine
Dab	2,4-Diaminobutyric Acid
DCM	Dichloromethane
DIC	N,N′-Di(propan-2-yl)methanediimine
DMF	N,N-Dimethylformamide
DOTA	2,2′,2″,2‴-(1,4,7,10-Tetraazacyclododecane-1,4,7,10-tetrayl) tetraacetic acid
DOTA-tris(tBu)-NHS	tri-tert-butyl 2,2′,2″-(10-(2-((2,5-dioxopyrrolidin-1-yl)oxy)-2-oxoethyl)-1,4,7,10-tetraazacyclododecane-1,4,7-triyl)triacetate
ESI-MS	Electrospray ionization mass spectrometry analyses
Et_3N	Triethylamine
$E_{\beta max}$	Beta emitter with a maximum energy
Fmoc	9-fluorenylmethoxycarbonyl group
hArg	Homoarginine
HCl	Hydrogen chloride
His	Histidine
HOBt	1H-1,2,3-Benzotriazol-1-ol
HS	Human Serum
IC_{50}	Half maximal inhibitory concentration
L	Lipophilicity
logP	Decimal logarithm of partition coefficient
m/z	Mass-to-charge ratio
mAb	Monoclonal antibodies
NH_2	Amino group
NRP-1	Neuropilin-1
P	Partition coefficient
Pbf	Pentamethyl-2,3-dihydrobenzofuran-5-sulfonyl group
PBS	Phosphate-buffered saline
PhOH	Phenol
$PhSiH_3$	Phenylsilane
RP-HPLC	Reverse-Phase High Pressure Liquid Chromatography
R_T	Retention time
RTKs	Receptor Tyrosine Kinases
SD	Standard deviation
SH	Thiol group
SPPS	Solid Phase Peptide Synthesis
$t_{1/2}$	Half-life time
TFA	Trifluoroacetic acid
TIPS	Tri(propan-2-yl)silane
VEGF	Vascular Endothelial Growth Factor
$VEGF-A_{165}$	Vascular Endothelial Growth Factor-A_{165}
VEGFR	Vascular Endothelial Growth Factor Receptor
VEGFR-2	Vascular Endothelial Growth Factor Receptor 2
Σ	sigma; operator for summation

References

1. Ferrara, N. Role of vascular endothelial growth factor in regulation of physiological angiogenesis. *Am. J. Physiol. Cell Physiol.* **2001**, *280*, 1358–1366. [CrossRef]
2. Ferrara, N.; Gerber, H.P.; LeCouter, J. The biology of VEGF and its receptors. *Nat. Med.* **2003**, *9*, 669–676. [CrossRef] [PubMed]
3. Grünewald, F.S.; Prota, A.E.; Giese, A.; Ballmer-Hofer, K. Structure–function analysis of VEGF receptor activation and the role of coreceptors in angiogenic signaling. *BBA—Proteins Proteom.* **2010**, *1804*, 567–580. [CrossRef] [PubMed]
4. Djordjevic, S.; Driscoll, P.C. Targeting VEGF signalling via the neuropilin co-receptor. *Drug Discov. Today* **2013**, *18*, 447–455. [CrossRef] [PubMed]
5. Roskoski, R., Jr. Vascular endothelial growth factor (VEGF) signaling in tumor progression. *Crit. Rev. Oncol. Hematol.* **2007**, *62*, 179–213. [CrossRef]
6. Soker, S.; Fidder, H.; Neufeld, G.; Klagsbrun, M. Characterization of Novel Vascular Endothelial Growth Factor (VEGF) Receptors on Tumor Cells That Bind VEGF165 via Its Exon 7-encoded Domain. *J. Biol. Chem.* **1996**, *271*, 5761–5767. [CrossRef]
7. Goel, H.L.; Mercurio, A.M. VEGF targets the tumour cell. *Nat. Rev. Cancer* **2013**, *13*, 871–882. [CrossRef]
8. Masłowska, K.; Halik, P.K.; Tymecka, D.; Misicka, A.; Gniazdowska, E. The Role of VEGF receptors as molecular target in nuclear medicine for cancer diagnosis and combination therapy. *Cancers* **2021**, *13*, 1072. [CrossRef]
9. Guo, H.F.; Vander Kooi, C.W. Neuropilin functions as an essential cell surface receptor. *J. Biol. Chem.* **2015**, *290*, 29120–29126. [CrossRef]
10. Soker, S.; Takashima, S.; Miao, H.Q.; Neufeld, G.; Klagsbrun, M. Neuropilin-1 is expressed by endothelial and tumor cells as an isoform-specific receptor for vascular endothelial growth factor. *Cell* **1998**, *92*, 735–745. [CrossRef]
11. Latil, A.; Bieche, I.; Pesche, S.; Valeri, A.; Fournier, G.; Cussenot, O.; Lidereau, R. VEGF overexpression in clinically localized prostate tumors and neuropilin-1 overexpression in metastatic forms. *Int. J. Cancer* **2000**, *89*, 167–171. [CrossRef]
12. Stephenson, J.M.; Banerjee, S.; Saxena, N.K.; Cherian, R.; Banerjee, S.K. Neuropilin-1 is differentially expressed in myoepithelial cells and vascular smooth muscle cells in preneoplastic and neoplastic human breast: A possible marker for the progression of breast cancer. *Int. J. Cancer* **2002**, *101*, 409–414. [CrossRef] [PubMed]
13. Parikh, A.A.; Liu, W.B.; Fan, F.; Stoeltzing, O.; Reinmuth, N.; Bruns, C.J.; Bucana, C.D.; Evans, D.B.; Ellis, L.M. Expression and regulation of the novel vascular endothelial growth factor receptor neuropilin-1 by epidermal growth factor in human pancreatic carcinoma. *Cancer* **2003**, *98*, 720–729. [CrossRef]
14. Parikh, A.A.; Fan, F.; Liu, W.B.; Ahmad, S.A.; Stoeltzing, O.; Reinmuth, N.; Bielenberg, D.; Bucana, C.D.; Klagsburn, M.; Ellis, L.M. Neuropilin-1 in human colon cancer: Expression, regulation, and role in induction of angiogenesis. *Am. J. Pathol.* **2004**, *164*, 2139–2151. [CrossRef]
15. Jubb, A.M.; Strickland, L.A.; Liu, S.D.; Mak, J.; Schmidt, M.; Koeppen, H. Neuropilin-1 expression in cancer and development. *J. Pathol.* **2012**, *226*, 50–60. [CrossRef] [PubMed]
16. Grandclement, C.; Borg, C. Neuropilins: A new target for cancer therapy. *Cancers* **2011**, *3*, 1899–1928. [CrossRef] [PubMed]
17. Puszko, A.K.; Sosnowski, P.; Pułka-Ziach, K.; Hermine, O.; Hopfgartner, G.; Lepelletier, Y.; Misicka, A. Urea moiety as amide bond mimetic in peptide-like inhibitors of VEGF-A165/NRP-1 complex. *Bioorganic Med. Chem. Lett.* **2019**, *29*, 2493–2497. [CrossRef]
18. Bagri, A.; Tessier-Lavigne, M.; Watts, R.J. Neuropilins in tumor biology. *Clin. Cancer Res.* **2009**, *15*, 1860–1864. [CrossRef]
19. Soker, S.; Gollamudi-Payne, S.; Fidder, H.; Charmahelli, H.; Klagsbrun, M. Inhibition of vascular endothelial growth factor (VEGF)-induced endothelial cell proliferation by a peptide corresponding to the exon 7-encoded domain of VEGF165. *J. Biol. Chem.* **1997**, *272*, 31582–31588. [CrossRef]
20. Cook, K.M.; Figg, W.D. Angiogenesis inhibitors: Current strategies and future prospects. *CA Cancer J. Clin.* **2010**, *60*, 222–243. [CrossRef]
21. Kiselyov, A.; Balakin, K.V.; Tkachenko, S.E. VEGF/VEGFR signalling as a target for inhibiting angiogenesis. *Expert Opin. Investig. Drugs* **2007**, *16*, 83–107. [CrossRef] [PubMed]
22. Tortora, G.; Melisi, D.; Ciardiello, F. Angiogenesis: A target for cancer therapy. *Curr. Pharm. Des.* **2004**, *10*, 11–26. [CrossRef] [PubMed]
23. Rüegg, C.; Hasmim, M.; Lejeune, F.J.; Alghisi, G.C. Antiangiogenic peptides and proteins: From experimental tools to clinical drugs. *Biochim. Biophys. Acta* **2006**, *1765*, 155–177. [CrossRef] [PubMed]
24. Murukesh, N.; Dive, C.; Jayson, G.C. Biomarkers of angiogenesis and their role in the development of VEGF inhibitors. *Br. J. Cancer* **2010**, *102*, 8–18. [CrossRef]
25. Peng, K.; Bai, Y.; Zhu, Q.; Hu, B.; Xu, Y. Targeting VEGF–neuropilin interactions: A promising antitumor strategy. *Drug Discov. Today* **2019**, *24*, 656–664. [CrossRef] [PubMed]
26. Ferrara, N.; Hillan, K.J.; Gerber, H.P.; Novotny, W. Discovery and development of bevacizumab, an anti-VEGF antibody for treating cancer. *Nat. Rev. Drug Discov.* **2004**, *3*, 391–400. [CrossRef]
27. Zhao, Y.; Adjei, A.A. Targeting angiogenesis in cancer therapy: Moving beyond vascular endothelial growth factor. *Oncologist* **2015**, *20*, 660–673. [CrossRef] [PubMed]
28. Jayson, G.C.; Zweit, J.; Jackson, A.; Mulatero, C.; Julyan, P.; Ranson, M.; Broughton, L.; Wagstaff, J.; Hakannson, L.; Groenewegen, G.; et al. Molecular imaging and biological evaluation of HuMV833 anti-VEGF antibody: Implications for trial design of antiangiogenic antibodies. *J. Natl. Cancer Inst.* **2002**, *94*, 1484–1493. [CrossRef] [PubMed]

29. Lu, X.; Fu Wang, R. A concise review of current radiopharmaceuticals in tumor angiogenesis imaging. *Curr. Pharm. Des.* **2012**, *18*, 1032–1040. [CrossRef] [PubMed]

30. Christoforidis, J.B.; Briley, K.; Binzel, K.; Bhatia, P.; Wei, L.; Kumar, K.; Knopp, M.V. Systemic biodistribution and intravitreal pharmacokinetic properties of bevacizumab, ranibizumab, and aflibercept in a nonhuman primate model. *Invst. Ophthalmol. Vis. Sci.* **2017**, *58*, 5636–5645. [CrossRef] [PubMed]

31. Backer, M.V.; Backer, J.M. Imaging key biomarkers of tumor angiogenesis. *Theranostics* **2012**, *2*, 502–515. [CrossRef] [PubMed]

32. Féliz, L.R.; Tsimberidou, A.M. Anti-vascular endothelial growth factor therapy in the era of personalized medicine. *Cancer Chemother. Pharmacol.* **2013**, *72*, 1–12. [CrossRef]

33. Kniess, T. Radiolabeled small molecule inhibitors of VEGFR-recent advances. *Curr. Pharm. Des.* **2012**, *18*, 2867–2874. [CrossRef]

34. Binétruy-Tournaire, R.; Demangel, C.; Malavaud, B.; Vassy, R.; Rouyre, S.; Kraemer, M.; Plouët, J.; Derbin, C.; Perret, G.; Mazie, J.C. Identification of a peptide blocking vascular endothelial growth factor (VEGF)-mediated angiogenesis. *EMBO J.* **2000**, *19*, 1525–1533. [CrossRef] [PubMed]

35. Starzec, A.; Vassy, R.; Martin, A.; Lecouvey, M.; Di Benedetto, M.; Crépin, M.; Perret, G.Y. Antiangiogenic and antitumor activities of peptide inhibiting the vascular endothelial growth factor binding to neuropilin-1. *Life Sci.* **2006**, *79*, 2370–2381. [CrossRef]

36. Teesalu, T.; Sugahara, K.N.; Kotamraju, V.R.; Ruoslahti, E. C-end rule peptides mediate neuropilin-1-dependent cell, vascular, and tissue penetration. *Proc. Natl. Acad. Sci. USA* **2009**, *106*, 16157–16162. [CrossRef]

37. Jarvis, A.; Allerston, C.K.; Jia, H.; Herzog, B.; Garza-Garcia, A.; Winfield, N.; Ellard, K.; Aqil, R.; Lynch, R.; Chapman, C.; et al. Small molecule inhibitors of the neuropilin-1 vascular endothelial growth factor A (VEGF-A) interaction. *J. Med. Chem.* **2010**, *53*, 2215–2226. [CrossRef] [PubMed]

38. Fedorczyk, B.; Lipiński, P.F.; Puszko, A.K.; Tymecka, D.; Wilenska, B.; Dudka, W.; Perret, G.Y.; Misicka, A. Triazolopeptides inhibiting the interaction between neuropilin-1 and vascular endothelial growth factor-165. *Molecules* **2019**, *24*, 1756. [CrossRef] [PubMed]

39. Puszko, A.K.; Sosnowski, P.; Rignault-Bricard, R.; Hermine, O.; Hopfgartner, G.; Pułka-Ziach, K.; Lepelletier, Y.; Misicka, A. Urea-Peptide Hybrids as VEGF-A165/NRP-1 Complex Inhibitors with Improved Receptor Affinity and Biological Properties. *Int. J. Mol. Sci.* **2021**, *22*, 72. [CrossRef]

40. Puszko, A.K.; Sosnowski, P.; Raynaud, F.; Hermine, O.; Hopfgartner, G.; Lepelletier, Y.; Misicka, A. Does Cysteine Rule (CysR) Complete the CendR Principle? Increase in Affinity of Peptide Ligands for NRP-1 Through the Presence of N-Terminal Cysteine. *Biomolecules* **2020**, *10*, 448. [CrossRef]

41. Puszko, A.K.; Sosnowski, P.; Tymecka, D.; Raynaud, F.; Hermine, O.; Lepelletier, Y.; Misicka, A. Neuropilin-1 peptide-like ligands with proline mimetics, tested using the improved chemiluminescence affinity detection method. *Medchemcomm* **2019**, *10*, 332–340. [CrossRef]

42. Grabowska, K.; Puszko, A.K.; Lipiński, P.F.; Laskowska, A.K.; Wileńska, B.; Witkowska, E.; Misicka, A. Design, synthesis and in vitro biological evaluation of a small cyclic peptide as inhibitor of vascular endothelial growth factor binding to neuropilin-1. *Bioorganic Med. Chem. Lett.* **2016**, *26*, 2843–2846. [CrossRef] [PubMed]

43. Tymecka, D.; Puszko, A.K.; Lipiński, P.F.; Fedorczyk, B.; Wilenska, B.; Sura, K.; Perret, G.Y.; Misicka, A. Branched pentapeptides as potent inhibitors of the vascular endothelial growth factor 165 binding to Neuropilin-1: Design, synthesis and biological activity. *Eur. J. Med. Chem.* **2018**, *158*, 453–462. [CrossRef]

44. Tymecka, D.; Lipiński, P.F.; Fedorczyk, B.; Puszko, A.; Wileńska, B.; Perret, G.Y.; Misicka, A. Structure-activity relationship study of tetrapeptide inhibitors of the Vascular Endothelial Growth Factor A binding to Neuropilin-1. *Peptides* **2017**, *94*, 25–32. [CrossRef] [PubMed]

45. Grabowska, K.; Puszko, A.K.; Lipiński, P.F.; Laskowska, A.K.; Wileńska, B.; Witkowska, E.; Perret, G.Y.; Misicka, A. Structure-activity relationship study of a small cyclic peptide Hc[Lys-Pro-Glu]-Arg-OH: A potent inhibitor of Vascular Endothelial Growth Factor interaction with Neuropilin-1. *Bioorganic Med. Chem.* **2017**, *25*, 597–602. [CrossRef]

46. Fedorczyk, B.; Lipiński, P.F.; Tymecka, D.; Puszko, A.K.; Wilenska, B.; Perret, G.Y.; Misicka, A. Conformational latitude–activity relationship of KPPR tetrapeptide analogues toward their ability to inhibit binding of vascular endothelial growth factor 165 to neuropilin-1. *J. Pept. Sci.* **2017**, *23*, 445–454. [CrossRef]

47. Starzec, A.; Ladam, P.; Vassy, R.; Badache, S.; Bouchemal, N.; Navaza, A.; du Penhoat, C.H.; Perret, G.Y. Structure-function analysis of the antiangiogenic ATWLPPR peptide inhibiting VEGF165 binding to neuropilin-1 and molecular dynamics simulations of the ATWLPPR/neuropilin-1 complex. *Peptides* **2007**, *28*, 2397–2402. [CrossRef]

48. Maleki, F.; Farahani, A.M.; Rezazedeh, F.; Sadeghzadeh, N. Structural modifications of amino acid sequences of radiolabeled peptides for targeted tumor imaging. *Bioorganic Chem.* **2020**, *99*, 103802. [CrossRef]

49. Rich, D.H.; Singh, J. The carbodiimide method. In *The Peptides: Analysis, Synthesis, Biology, Volume 1: Major Methods of Peptide*; Gross, E., Meienhofer, J., Eds.; Academic Press: New York, NY, USA, 1979; Volume 1, pp. 241–261. [CrossRef]

50. Kaiser, E.; Colescott, R.L.; Bossinger, C.D.; Cook, P.I. Color test for detection of free terminal amino groups in the solid-phase synthesis of peptides. *Anal. Biochem.* **1970**, *34*, 595–598. [CrossRef]

51. Christensen, T. Qualitative test for monitoring coupling completeness in solid phase peptide synthesis using chloranil. *Acta Chem. Scand. B* **1979**, *33*, 763–766. [CrossRef]

52. Izdebski, J.; Witkowska, E.; Kunce, D.; Orłowska, A.; Baranowska, B.; Radzikowska, M.; Smoluch, M. New potent hGH-RH analogues with increased resistance to enzymatic degradation. *J. Pept. Sci.* **2002**, *8*, 289–296. [CrossRef] [PubMed]

53. Thieriet, N.; Alsina, J.; Giralt, E.; Guibé, F.; Albericio, F. Use of Alloc-amino Acids in Solid-Phase Peptide Synthesis. Tandem Deprotection-Coupling Reactions Using Neutral Conditions. *Tetrahedron Lett.* **1997**, *38*, 7275–7278. [CrossRef]

54. Gillings, N.; Hjelstuen, O.; Ballinger, J.; Behe, M.; Decristoforo, C.; Elsinga, P.; Ferrari, V.; Peitl, P.K.; Koziorowski, J.; Laverman, P.; et al. Guideline on current good radiopharmacy practice (cGRPP) for the small-scale preparation of radiopharmaceuticals. *EJNMMI Radiopharm. Chem.* **2021**, *6*, 8. [CrossRef] [PubMed]

55. European Medicines Agency Guideline on the Non-Clinical Requirements for Radiopharmaceuticals. Available online: https://www.ema.europa.eu/en/documents/scientific-guideline/draft-guideline-non-clinical-requirements-radiopharmaceuticals-first-version_en.pdf (accessed on 14 December 2021).

56. Balani, S.K.; Miwa, G.T.; Gan, L.-S.; Wu, J.-T.; Lee, F.W. Strategy of Utilizing In Vitro and In Vivo ADME Tools for Lead Optimization and Drug Candidate Selection. *Curr. Top. Med. Chem.* **2005**, *5*, 1033–1038. [CrossRef] [PubMed]

57. Tibbitts, J.; Canter, D.; Graff, R.; Smith, A.; Khawil, L.A. Key factors influencing ADME properties of therapeutic proteins: A need for ADME characterization in drug discovery and development. *mAbs* **2016**, *8*, 229–245. [CrossRef]

58. Doogue, M.P.; Polasek, T.M. The ABCD of clinical pharmacokinetics. *Ther. Adv. Drug Saf.* **2013**, *4*, 5–7. [CrossRef]

59. Nelson, E. Kinetics of drug absorption, distribution, metabolism, and excretion. *J. Pharm. Sci.* **1961**, *50*, 181–192. [CrossRef]

60. Hansch, C.; Clayton, J.M. Lipophilic character and biological activity of drugs II: The parabolic case. *J. Pharm. Sci.* **1973**, *62*, 1–21. [CrossRef]

61. Waterhouse, R.N. Determination of lipophilicity and its use as a predictor of blood–brain barrier penetration of molecular imaging agents. *Mol. Imaging Biol.* **2003**, *5*, 376–389. [CrossRef]

62. Waring, M.J. Lipophilicity in drug discovery. *Expert Opin. Drug Discov.* **2010**, *5*, 235–248. [CrossRef] [PubMed]

63. Arnott, J.A.; Planey, S.L. The influence of lipophilicity in drug discovery and design. *Expert Opin. Drug Discov.* **2012**, *7*, 863–875. [CrossRef]

64. Rutkowska, E.; Pajak, K.; Jóźwiak, K. Lipophilicity–methods of determination and its role in medicinal chemistry. *Acta Pol. Pharm.* **2013**, *70*, 3–18. [PubMed]

65. Chung, T.D.Y.; Terry, D.B.; Smith, L.H.; Markossian, S.; Grossman, A.; Brimacombe, K.; Arkin, M.; Auld, D.; Austin, C.P.; Baell, J.; et al. *In Vitro and In Vivo Assessment of ADME and PK Properties During Lead Selection and Lead Optimization—Guidelines, Benchmarks and Rules of Thumb*; Eli Lilly & Company and the National Center for Advancing Translational Sciences: Bethesda, ML, USA, 2004. Available online: https://www.ncbi.nlm.nih.gov/books/NBK326710/ (accessed on 17 December 2021).

66. Pike, V. Radiotracers: Crossing the blood-brain barrier and surviving metabolism. *Trends Pharmacol. Sci.* **2009**, *30*, 431–440. [CrossRef] [PubMed]

67. Misra, A.; Ganesh, S.; Shahiwala, A.; Shah, S.P. Drug delivery to the central nervous system: A review. *J. Pharm Pharm. Sci.* **2003**, *6*, 252–273. [PubMed]